Received: 13 January 2026 Accepted: 17 January 2026 Published Date: 29 January 2026

ScienceFrontier

Research Article

International Social Science Research and Review

ISSN Online: 3067-9680 | OPEN ACCESS

Sensitivity of Bacillus Cereus Isolates from Clinical Sources and Compatibility of Zno Nanoparticles with Tetracycline Antibiotics

Moammal F. Hawad *| Mohsin Hashim Risan| M. Alili

Department of applied biology, College of biotechnology, Al-Nahrain University, Baghdad, Iraq.

***Corresponding Author:** Moammal F. Hawad, *Department of applied biology, College of biotechnology, Al-Nahrain University, Baghdad, Iraq*

Citation: Moammal F. Hawad , Mohsin Hashim Risan , M. Alili (2026) Sensitivity of Bacillus Cereus Isolates from Clinical Sources and Compatibility of Zno Nanoparticles with Tetracycline Antibiotics, J International Social Science Research and Review; 3 (1) 22, **DOI:** https://doi.org/10.5281/zenodo.21776006

Abstract:

Bacillus cereus is an important foodborne pathogen and a significant public health concern owing to its ability to produce highly resistant endospores and the increasing emergence of multidrug-resistant strains. This study evaluated the prevalence and antimicrobial susceptibility profiles of B. cereus isolates recovered from clinical and investigated the antibacterial activity of biogenic zinc oxide nanoparticles (ZnO-NPs) against these isolates. The eleven B. cereus isolates represented a prevalence of 36.6% and exhibited high levels of resistance to β-lactam antibiotics and trimethoprim, with sensitivity to antibiotics from a panel of 8 antibiotics, including vancomycin (30 µg), Imipenem (10 µg), Meropenem (10 µg), Amikacin (30 µg), Ciprofloxacin (5 µg), Levofloxacin (5 µg), Tetracycline (30 µg), and Trimethoprim (5 µg). The inhibition zone measurement was interpreted by (CLSI, 2023) Biogenic ZnO-NPs were synthesized through an environmentally friendly method using Moringa oleifera leaf extract and characterized using X-ray diffraction (XRD), field emission scanning electron microscopy (FESEM), atomic force microscopy (AFM), and Fourier transform infrared spectroscopy (FTIR). The characterization confirmed the successful synthesis of semi-crystalline, spherical ZnO nanoparticles with grain sizes ranging from 37.93 to 78.39 nm. Antibacterial assays demonstrated that biogenic ZnO-NPs exhibited significant antibacterial activity against B. cereus, with the greatest inhibitory effect observed at a concentration of 5 mg/mL. Furthermore, the combination of ZnO-NPs with tetracycline significantly enhanced the antibacterial activity of tetracycline compared with the antibiotic alone. Previously resistant isolates became susceptible following combination treatment, an effect that may be attributed to ZnO-NP-induced alterations in the bacterial cell envelope, increased membrane permeability, and possible interference with efflux-mediated resistance mechanisms, thereby facilitating greater intracellular accumulation of tetracycline. Overall, these findings suggest that biogenic ZnO-NPs may serve as promising antibacterial adjuvants capable of enhancing the efficacy of conventional antibiotics against resistant B. cereus isolates and may contribute to future strategies aimed at combating antimicrobial resistance.

Key words:

bacillus cereus;

green synthesis;

zinc oxide nanoparticles;

moringa oleifera;

synergistic efficacy

Introduction:

Bacillus cereus is a Gram-positive spore-forming bacterium that is found in various environments including soil, food products, and food processing plants.*Bacillus cereus* is capable of producing extremely resistant endospores which allow it to survive under harsh conditions,

e.g. high temperature, dryness and exposure to chemicals (Woh *et al*., 2024).
Nanotechnology is the manipulation of materials on a nanoscopic scale (1-100 nm), where the innate properties of materials differ grossly from the properties of these large area materials. Because nanomaterials have high surface area-to-volume ratios; low molecular weights, tunable surface chemistry; and enhanced reactivity, they have become a vital component of developments in nearly every area of science and the industrial world, including medicine, biotechnology, pharmaceuticals, agriculture, and environmental science (Rao *et al*., 2021). Zinc oxide nanoparticles (ZnO-NPs) are one type of several different types of nanomaterials being analysed for their antimicrobial effect; they have received a lot of interest as they have been proven to have an excellent safety record, are generally inexpensive to produce and show potency against a large variety of bacteria, including Gram-positive bacteria like *Bacillus cereus*, as documented by recent studies (Mohammed *et al*., 2025; Al-Mashhadani, 2025).

In addition to the antibacterial properties of ZnO-NPs, many researchers are investigating the use of ZnO-NPs produced from the biosynthesis of plant extracts or biological processes as they exhibit very good enzyme-inhibiting activity against Gram-positive bacteria due to enhanced production of reactive oxygen species and increased surface area to contact the bacteria (Al-Mashhadani, 2025; Mohammed *et al*., 2025).The manufacture of zinc oxide nanoparticles was studied using analytical techniques such as UV-visible spectroscopy and XRD, along with imaging techniques like FE-SEM and AFM.The UV-Visible absorption scan of the supernatant infused with zinc chloride exhibited a peak at 36nm, signifying the surface plasmon resonance (SPR) of zinc oxide nanoparticles. (Jayachandran *et al*., 2021) (Hassan and Risan, 2024).

Material and Methods:

Sample collection

A total of 30 samples were collected during the period from October 2025 to January 2026. Clinical samples were collected from patients suffering from diarrhea or vomiting whose ages ranged between 10 years to 40 years from several hospitals in Baghdad: Baghdad Educational Hospital, Specialized burns Hospital, and Ghazi Hariri Hospital, performed by plating samples on selective agar media of *B. cereus*.

Isolation and Phenotypic Characterization

The initial step in isolating the samples was the use of Nutrient Agar and Blood Agar (to determine if the samples produced beta hemolysin). Selective isolation was performed using Polymyxin Pyruvate Egg Yolk Mannitol Bromothymol Blue Agar (PEMBA) to facilitate further studies on the bacterial isolates. The presence of B. cereus can be identified through the observation that B. cereus colonies are peacock blue in color they do not ferment mannitol (this is indicated by the blue color of the agar). they have a strong lecithinase activity (this manifests itself as a clear zone around the colonies on egg yolk). Isolated bacterial strains were subsequently tested to determine their metabolic and biochemical characteristics using the automated VITEK® 2 platform developed by (bioMérieux of France).

Antibiotic susceptibility Test

Antimicrobial susceptibility testing of *Bacillus cereus* from clinical isolates was done by using the Kirby–Bauer disk diffusion method according to CLSI (2023), Bacterial suspension equivalent to 0.5 McFarland (approximately 1.5×10^8 CFU/mL) was prepared from fresh cultures, and a sterile cotton swab was used to inoculate Mueller–Hinton agar plates in three directions to ensure uniform growth, after which the plates were allowed to dry for 3–5 minutes before applying antibiotic disks including Vancomycin (30 µg), Imipenem (10 µg), Meropenem (10 µg), Amikacin (30 µg), Ciprofloxacin (5 µg), Levofloxacin (5 µg), Tetracycline (30 µg), and Trimethoprim (5 µg) as a single agent were commercially obtained (biobase Canada). These antibiotics were selected to represent clinically relevant agents against Gram-positive and spore-forming bacteria. followed by incubation at 37°C for 24hours inhibition zone diameters measured and interpreted as susceptible, intermediate, or resistant according to CLSI standards (CLSI, 2023; Humphries et al., 2021),

Preparation of moringa plant extract

Fresh leaves of Moringa oleifera were thoroughly washed with distilled water to remove surface contaminants and then shade-dried at room temperature for 24 hours until complete drying was achieved. The dried leaves (50 g, dry weight) were mechanically homogenized with 500 mL of sterile distilled water (1:10 w/v) using a high speed blender for 5 minutes following the method described by (Elumalai *et al*,2015). The resulting homogenate was filtered through Whatman No. 1 filter paper, and the filtrate was further clarified by centrifugation at 8000 rpm for 15 minutes (Moodley *et al*., 2018) to obtain a clear, particle-free extract. The prepared extract was stored at 4 °C a for the subsequent green synthesis of zinc oxide nanoparticles.

Preparation of ZnO Nanoparticles

15g of zinc chloride were gradually added to 300 mL of Moringa oleifera leaf extract under continuous stirring. The reaction mixture was mechanically stirred at 500–600 rpm and heated at 70 °C for 3 hours to facilitate the formation of zinc oxide nanoparticle precursors. The pH of the solution was adjusted to 10 to promote the formation of zinc hydroxide as an intermediate for ZnO nanoparticle synthesis (Jadoun *et al*.,2021). The reaction mixture was then allowed to stabilize for 24 hours in the dark. The resulting precipitate was collected by centrifugation at 8000 rpm for 20 minutes at 4 °C, washed twice with absolute ethanol (Moodley et al., 2018), and dried at oven in 60°C. The dried product was further subjected to thermal treatment to obtain ZnO nanoparticles. All experiments were performed in triplicate to ensure reproducibility. Appropriate control groups were included, comprising a negative control (sterile saline), plant extract control, zinc chloride solution control, ZnO nanoparticles alone, and antibiotic-only control, in order to accurately evaluate the antibacterial activity and distinguish between individual and synergistic effects (Banoee *et al*., 2010; Jadoun *et al*., 2021).

Results and Discussion:

The isolation protocol revealed that 36.6% (or 11/30 confirmed isolates) were recovered. Moreover, confirmed isolates grown on PEMBA agar had 100% specificity and inhibited the growth of any other potentially competitive microflora. The confirmed isolates had good lecithinase production and beta-hemolysis showed they had pathogenic potential.

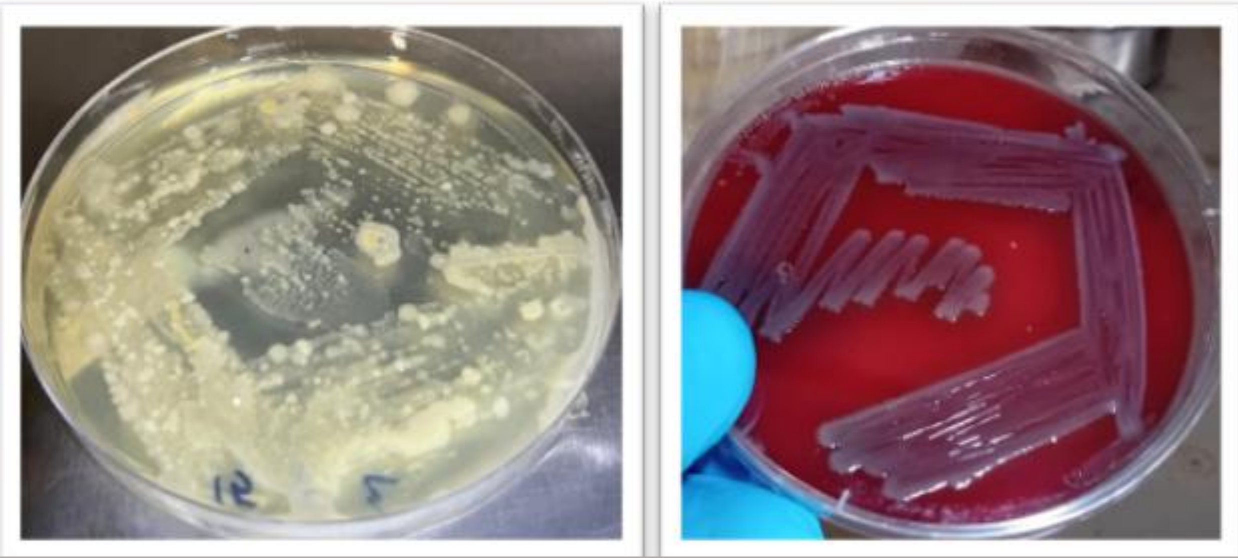

a) colony on Nuttrient agar ***b) colony on Blood agar***

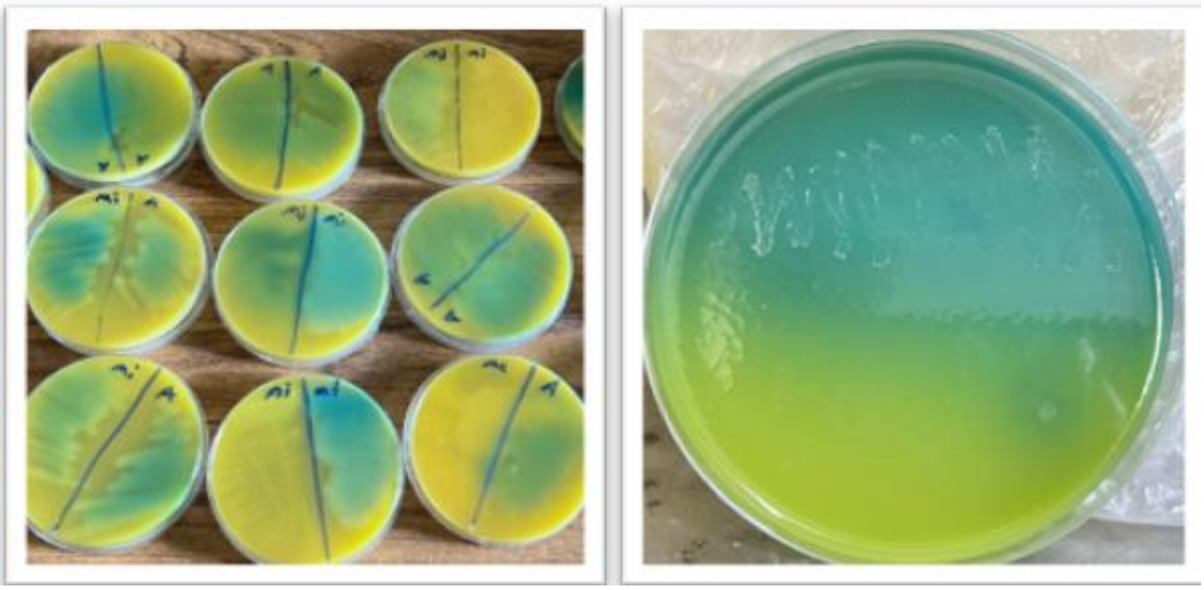

c) colony on PEMBA agar

Figure (1): *Colony Morphology and Cultural Characteristics of Bacillus cereus Isolates.*

Vitek-2 System:

the isolates were identified as Bacillus cereus with high confidence using theVITEK®2 automated identification system (Fig 2).

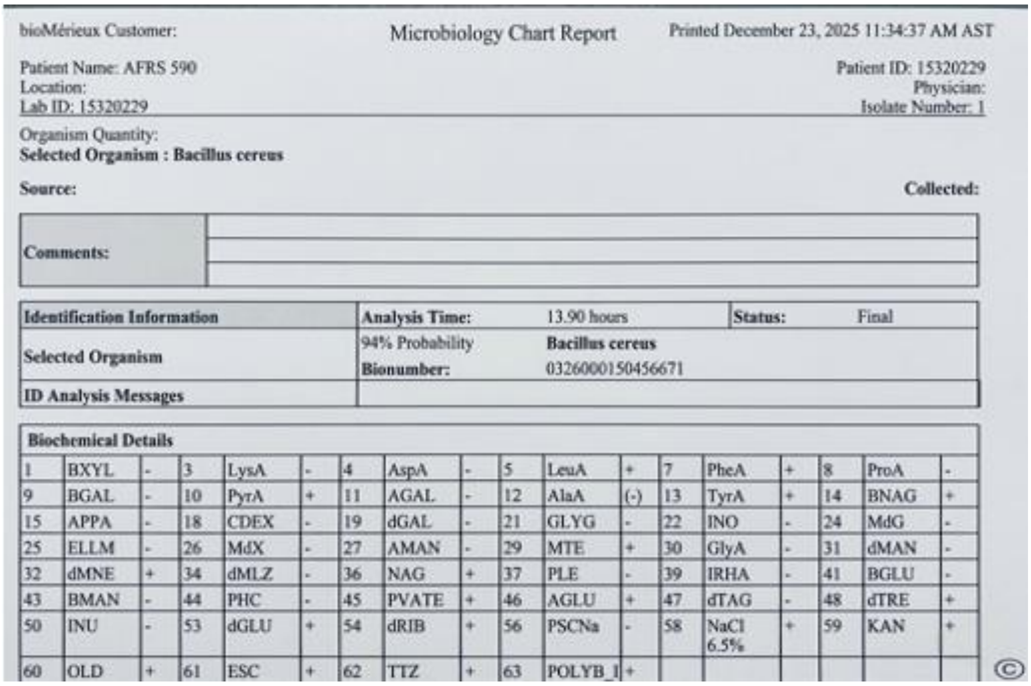

bioMérieux Customer: | Microbiology Chart Report | Printed December 23, 2025 11:34:37 AM AST

Patient Name: AFRS 590
Location:
Lab ID: 15320229

Patient ID: 15320229
Physician:
Isolate Number: 1

Organism Quantity:
Selected Organism : Bacillus cereus

Source: **Collected:**

Comments:	

Identification Information	**Analysis Time:** 13.90 hours	**Status:** Final
Selected Organism	94% Probability **Bacillus cereus** **Bionumber:** 0326000150456671	
ID Analysis Messages		

Biochemical Details

1	BXYL	-	3	LysA	-	4	AspA	-	5	LeuA	+	7	PheA	+	8	ProA	-
9	BGAL	-	10	PyrA	+	11	AGAL	-	12	AlaA	(-)	13	TyrA	+	14	BNAG	+
15	APPA	-	18	CDEX	-	19	dGAL	-	21	GLYG	-	22	INO	-	24	MdG	-
25	ELLM	-	26	MdX	-	27	AMAN	-	29	MTE	+	30	GlyA	-	31	dMAN	-
32	dMNE	+	34	dMLZ	-	36	NAG	+	37	PLE	-	39	IRHA	-	41	BGLU	-
43	BMAN	-	44	PHC	-	45	PVATE	+	46	AGLU	+	47	dTAG	-	48	dTRE	+
50	INU	-	53	dGLU	+	54	dRIB	+	56	PSCNa	-	58	NaCl 6.5%	+	59	KAN	+
60	OLD	+	61	ESC	+	62	TTZ	+	63	POLYB_R	+						

Figure (2): *B. cereus identification by VITEK 2 system.*

Antibiotic Susceptibility Test

Bacillus cereus was independently assessed for sensitivity to antibiotics from a panel of 8 antibiotics, including vancomycin (30 µg), Imipenem (10 µg), Meropenem (10 µg), Amikacin (30 µg), Ciprofloxacin (5 µg), Levofloxacin (5 µg), Tetracycline (30 µg), and Trimethoprim (5 µg). The inhibition zone measurement was interpreted by (CLSI, 2023) standards and the results were divided into 3 groups: Susceptible (S), Intermediate (I) or Resistant (R). All isolats of *Bacillus cereus* were moderately to highly susceptible to both carbapenems; both imipenem and meropenem; both fluoroquinolones; both ciprofloxacin and levofloxacin; vancomycin; amikacin; and tetracycline. All isolats of *Bacillus cereus* exhibited total resistance towards trimethoprim; The lack of susceptibility of *Bacillus cereus* to beta-lactam antibiotics; e.g., penicillin and ampicillin; may be a result of production of beta-lactamase enzymes (Maturin and Peeler,2001). antibiotic susceptibility patterns shwoen in table (1) and figure (3).

Clinical isolates

Clinical one distinctive isolate (m7) shwoed a relatively reduced susceptibility level compared to food-derived isolates. The inhibition zones for imipenem and meropenem were 30 mm and 22 mm, respectively, both interpreted as susceptible according to CLSI criteria The isolates remained susceptible to ciprofloxacin, levofloxacin, vancomycin, amikacin, and tetracycline, while complete resistance to trimethoprim was observed. The reduced susceptibility observed in clinical isolates may reflect prior exposure to antimicrobial agents. This results agree with (Ikeda *et al*., 2015) which report that *b.cereus* remain susceptible to carbapenems, fluoroquinolones, vancomycin, aminoglycosides, and tetracycline, while resistance to trimethoprim.

Antibiotic (µg)	Clinical isolate m7 (mm)
Vancomycin(30 µg)	20
Imipenem(10 µg)	30
Meropenem(10 µg)	22
Amikacin(30 µg)	21
Ciprofloxacin(5 µg)	26
Levofloxacin(5 µg)	22
Tetracycline(30 µg)	21
Trimethoprim(5 µg)	5

Table (1): *Antibiotic susceptibility patterns of clinical Bacillus cereus inhibition zone according to CLSI (2023)*

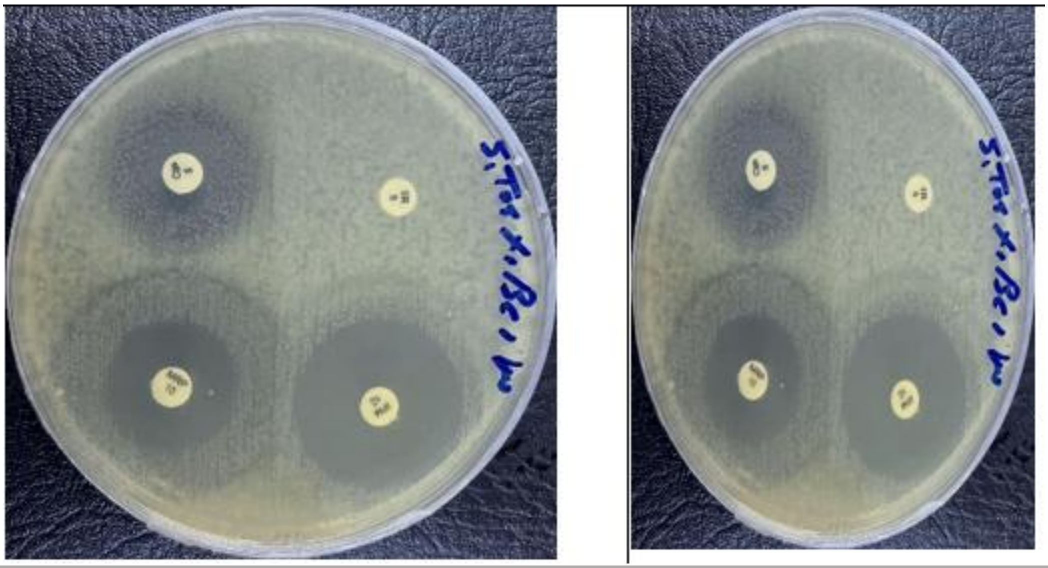

Figure (3): *Antibiotic susceptibility test of Bacillus cereus isolates on mueller –hinton agar*

Green Synthesis of ZnO Nanoparticles using Moringa Leaves Extract

Synthesizing nanoparticles using green methods enhances the rate of inhibition as compared to conventional delivery methods and also maintains the antimicrobial activity longer than traditional delivery methods. The presence of yellowish white precipitates in the solution combination proved the presence of the plant extract shown in figure (4).

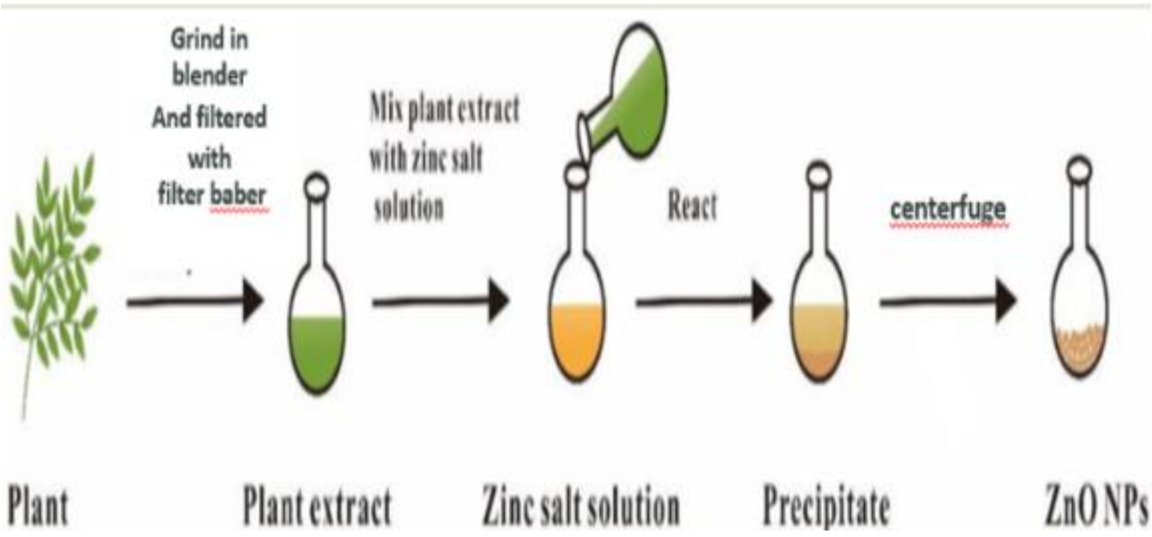

Figure (4): *Diagram of the manufacturing process for ZNO-NP.*

Characterization of ZnO-AV NPs

UV/Visible Spectral Analyses

The zinc oxide nanoparticle UV-Visible absorption spectrum showed intense absorption peak at 365 nm, exhibiting an absorbance of 0.850, this confirming the successful synthesis of ZnO nanoparticles. The characteristic excitonic peak at 365 nm is the result of the electronic transition of electrons from the valence band to the conduction band over the direct band gap of ZnO nanoparticles (Talam *et al*., 2012). The sharpness and symmetry of the absorption peak suggest a relatively uniform particle size distribution and low aggregation of the synthesized nanoparticles, whereas broad absorption bands are typically associated with particle agglomeration or non-uniform particle sizes.the UV-Vis spectrum indicates a gradual decrease in absorbance across the visible region confirming the high transparency and purity of the ZnO nanoparticles with minimal structural defects or impurities (Senthilkumar and Sivakumar, 2014). The absorption peak at 365 nm corresponds to a photon energy of approximately 3.40 eV according to relation.Calculated Optical Bandgap is slightly higher than that observed for ZnO due largely to a phenomenon known as blue shift that occurs from quantum confinement when particles are nanomaterials (Morkoç and Özgür, 2009). Evidence of this effect and related quantum size effects have also been reported by Zakak *et al*., (2011) who showed how reduced particle dimensions can result in a significant increase in optical properties and increased band gap energy for nanosized ZnO.

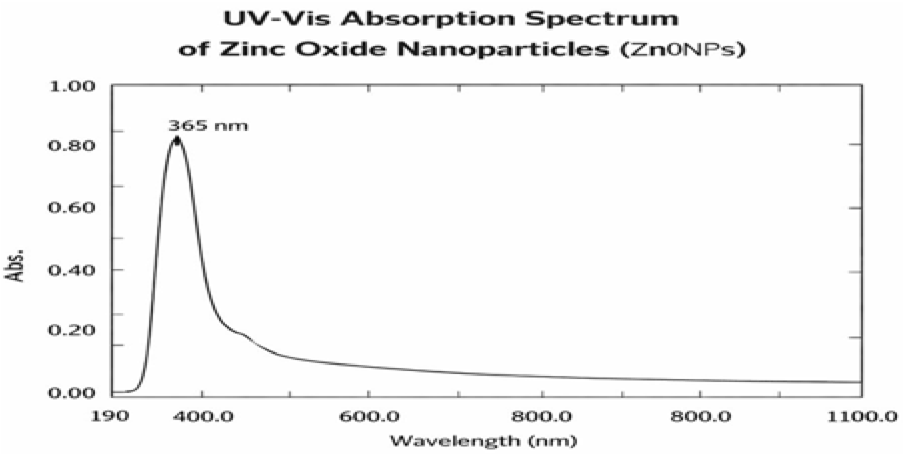

Peak Pick			
No.	P/V	Wavelength nm	Abs.
1	Peak	365.0	0.850

Figure (5): *The absorption spectrum of ZnO NPs*

Atomic Force Microscopy (AFM)

The surface topography and morphological characteristics of the prepared films were investigated using Atomic Force Microscopy (AFM). The surface exhibits a dense arrangement of self-assembled nanometric grains, the average surface roughness (Sa) was determined to be 311.11 pm, while the root mean square (RMS) roughness (Sq) was measured at 518.45 pm. The height distribution analysis indicates that the maximum peak height (Sp) reaches 781 pm, with a total vertical range (Z-axis) of approximately 1.77 nm. figure (5) illustrates the 2D and 3D AFM micrographs, which reveal a highly uniform and homogeneous distribution of nanostructures across the scanned area of (2.5 x2.5 µm). indicating a well-controlled growth process. Quantitative analysis of the surface roughness parameters provides precise insights into the film's quality. These measurements at the picometer scale signify an ultra-smooth surface with high structural integrity and minimal surface defects.

The minimal roughness values (less than 1 nm) align with the research of (Krysova *et al*., 2024), who demonstrated that high-density nanostructured films with low surface roughness exhibit superior structural and functional performance. This is also in agreement with (Maria and Rahman, 2025), who emphasized that such smooth morphologies and controlled grain growth are indicative of high crystallinity and a well-defined growth mechanism.

The high degree of smoothness and the organized arrangement of the nanostructures observed in this study are consistent with findings reported in recent literature for high-quality metal oxide thin films. According to (Toma *et al*., 2025), optimized deposition parameters lead to a uniform grain arrangement and a significant reduction in surface roughness, which is essential for enhancing functional properties. The observed topography confirms that the synthesis method successfully suppressed large-scale grain agglomeration, resulting in a more stable and uniform surface compared to conventional preparation techniques.

furthermore, the dense packing of the grains across the substrate confirms the efficiency of the synthesis process in producing high-quality nanostructured surfaces suitable for advanced applications.

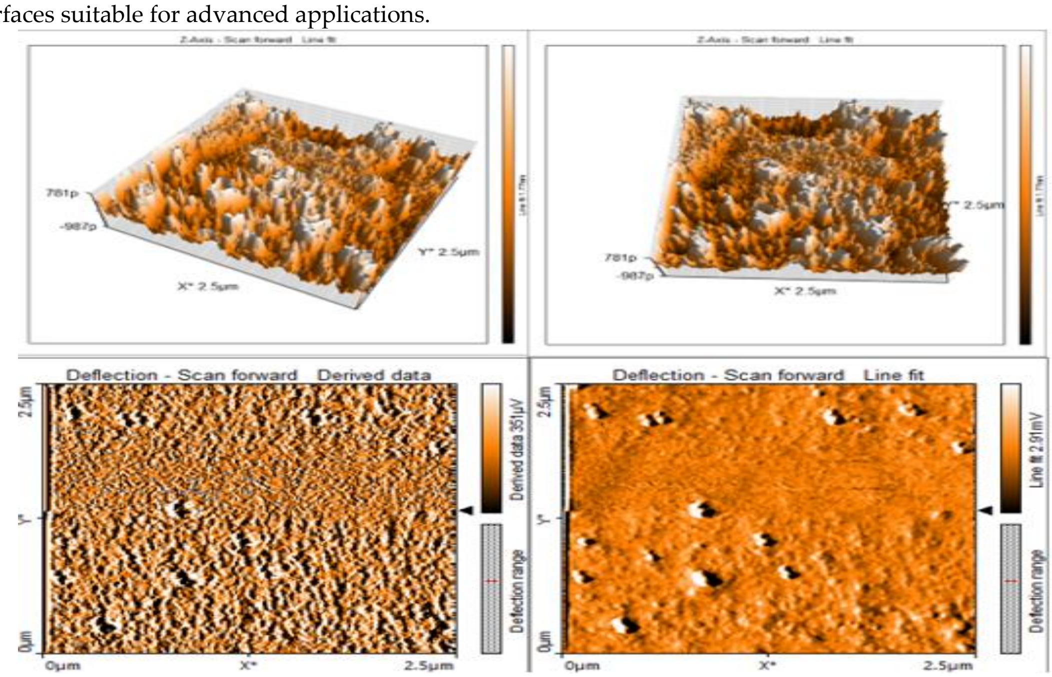

Figure (6): *AFM 3-dimensional image of Moringa ZnO NPs*

Fourier Transform Infra-Red Spectroscopy (FTIR) Test

The Fourier Transform Infrared (FTIR) spectroscopy is a powerful analytical tool for characterizing and synthesized ZNO nanoparticles and to identify the functional groups present in these compounds which help understand their molecular nature. The FT-IR spectra provide absorption peaks corresponding to the vibrational modes of the functional groups; therefore, different types of functional signature such as OH, C=O, N-H, C-H, can be detected. Thus it serves reliable evidence to help verify the presence of chemical bonds of interest within the samples (Verma *et al*., 2022). The FTIR spectra (Figure 6) of the as-prepared sample contain several characteristic absorption bands that provide insight into its chemical structure. The broad and intense absorption peak at approximately 3283cm^{-1} attributed to O-H stretching vibrations, the is expected due the presence of hydroxyl groups from either moisture or phenolic compounds that were involved in the stabilizing process. The peaks at 2962 cm^{-1}, 2920 cm^{-1} and 2851 cm^{-1} are due to asymmetric and symmetric C-H stretching vibrations associated with the aliphatic groups. The absorption band at 1627 cm^{-1} relates either to C=O stretching or to C=C skeletal vibrations. frequently found in proteins or flavonoids from plants used in the synthesis. Additionally, the presence of multiple peaks between 1540–1264 cm^{-1} indicates the presence of C-C stretching and C-H bending modes. The most significant feathure of the spectrum is the very strong absorption bands at lower wavenumbers (524, 457, and 422 cm^{-1}) are indicative of metal-oxygen (ZNO). These peak confirm the successful formation of an inorganic phase of the crystalline phase of the nanoparticles. The results obtained from FTIR spectral analysis verified that several functional groups contributed to both the reduction and stabilization of the nanoparticles. The broad spectral absorption band at 3283 cm^{-1} is attributed to the O–H stretching vibrations, which correlates with the results of Ahmed and Alias (2024). where phenolic hydroxyl functional groups were identfied as the primary reducing agents during the green synthesis.

The C–H stretching vibrations (2962 and 2851 cm^{-1}) agree with(Nakamoto, 2009).who identified aliphatic chains associated with organic capping layers that limit nanoparticles agglomeration. The intense peak of 1,627 cm^{-1} (Amide I), consist with the work (Abdellatif *et al*., 2023). which indicating flavonoids/proteins are responsible for the stabilization of metal oxide nanoparticles. The shift peak confirms the strong interaction between organic molecules and the nanoparticle surface. According to (Handore *et al*., 2014) these vibrational bands n the fingerprint region (524–422 cm^{-1}) represent the primary characteristics of crystalline metal oxide nanostructures confirming that the materials are present in a stable inorganic solid form.

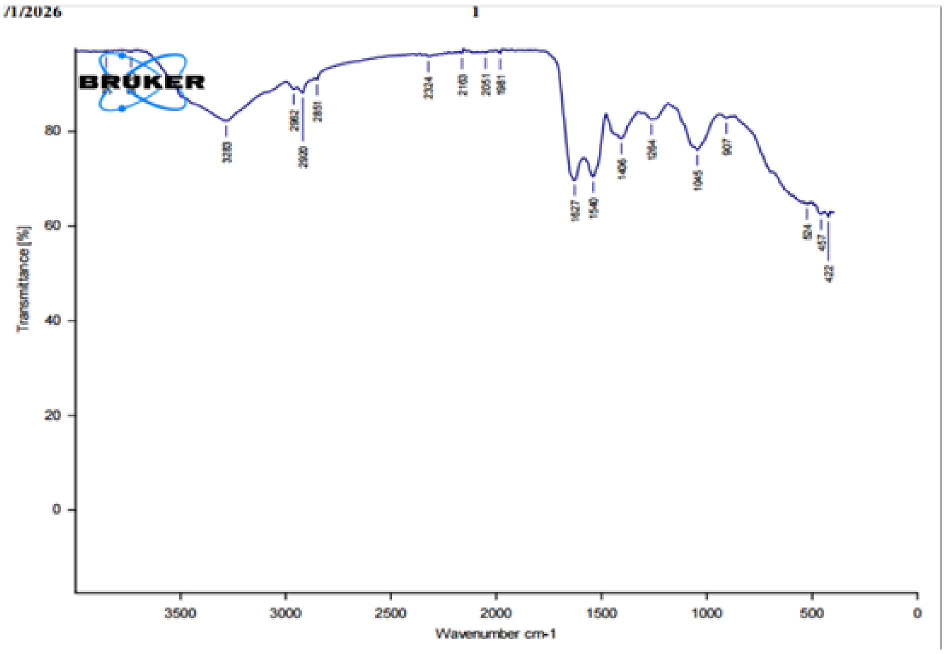

Figure (7): *The FT-IR spectrum of ZnO NPs*

Scanning Electron Microscopy Analysis:

Field Emission Scanning Electron Microscopy (FESEM) was used to characterize the morphology and determine the particle size distribution of the manufactured nanomaterials. As compared to standard scanning electron microscopy (SEM), FESEM produces improved resolution and imaging of nanostructures at low accelerating voltages. This is important because it enables observation of the fine porosity, and agglomeration state of material. In this study, FESEM was used to confirm that the transition from bulk precursors to nanometers occurred and to identify the structural features formed from the starting materials.The FESEM images show that the produced nanomaterials are composed primarily of densely aggregated nanoparticles with irregular shapes and a surface texture similar to that of an amorphous solid (Figure 8). The grain size analysis of the sample shows three clearly defined sizes of the nanoparticles (37.93 nm, 48.57 nm, and 78.39 nm). The morphology obtained in this study is consistent with the green synthesis methods described by (Radulescu et al., 2023). These authors point to the bio-derived stabilizers used as stabilizing agents producing these clustered structures. Additionally, the particle sizes measured (38-79 nm) are also in accordance with data reported by (Mtavangu *et al*,.2024). for ZnO nanocomposites produced using leaf extracts, confirming that the method used in the present study yields materials with the appropriate nanoscale dimensions for biomedical and environmental purposes.

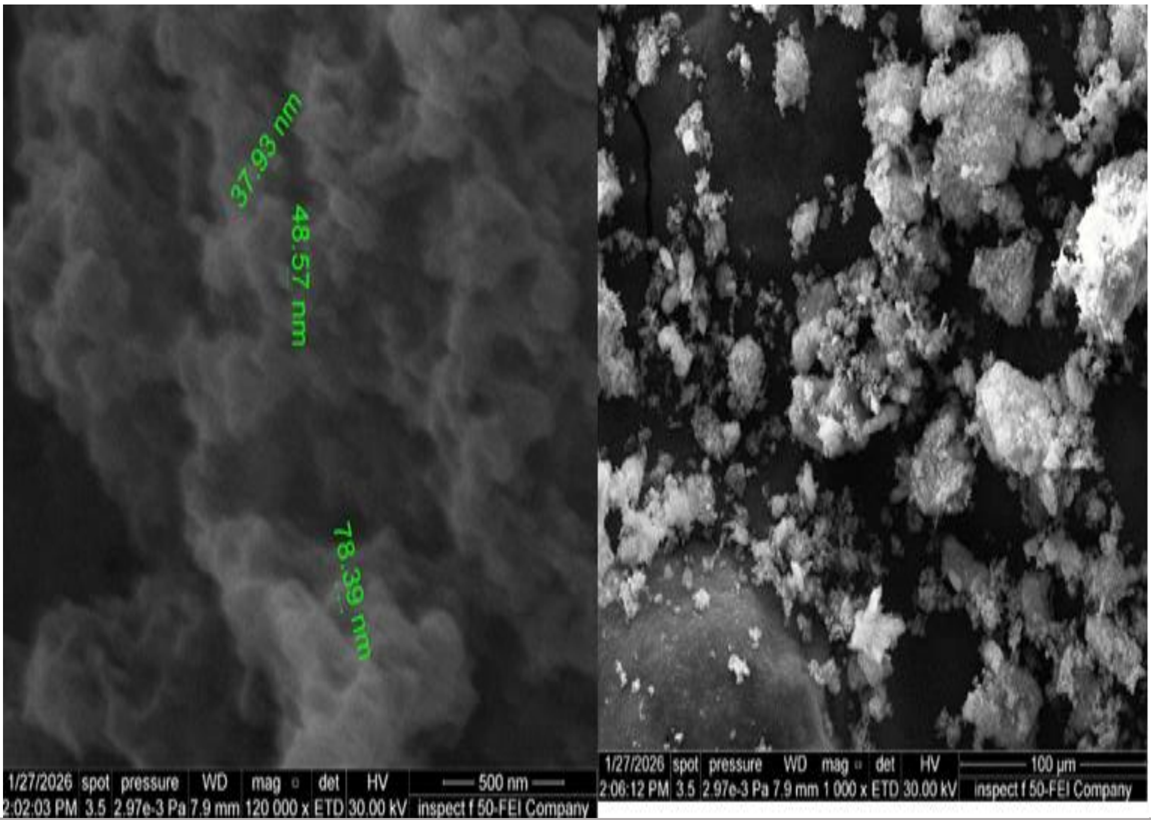

Figure (8): *The SEM image of ZnO nanoparticles*

X-Ray Diffraction

By using X-ray diffraction (XRD), The crystalline structure, phase purity, and crystallite size of the synthesized ZnO nanoparticles were characterized.figure (9),illustrate The XRD pattern. exhibits a series of diffraction peaks in the 2theta range of 10°–80°. The presence of intense and sharp peaks confirms the formation of a well-defined crystalline phase. The principal diffraction peaks observed at 2theta values of approximately 31.76°, 34.42°, and 36.25° correspond to the (100), (002), and (101) Miller indices (hkl), respectively. These peaks are in excellent agreement with the standard JCPDS card no. 36-1451, The sharpest peak observed at 33.45° and the presence of other significant peaks at 21.83° and 58.88° provide further evidence of the crystalline nature of the sample. confirming the hexagonal wurtzite structure of ZnO. A noticeable feature of the XRD profile is the broadening of the diffraction peaks, particularly the principal peak at 33.450 with a Full Width at Half Maximum (FWHM) of 1.46°. This peak broadening is a direct physical indicator of the nanoscale dimensions of the synthesized particles. To determine the average crystallite size (D), the Debye-Scherrer equation was applied D= K lambda\beta cos theta

Where K is the Scherrer constant (0.9), lambdais the X-ray wavelength (1.5406 for Cu-K alpha radiation), beta is the FWHM in radians, and theta is the Bragg angle. The calculated size confirms that the particles are within the nanometric range.The XRD profile exhibits a broad hump at lower angles (between 20° and 30°), which indicates the presence of an amorphous organic phase. This is a typical hallmark of green synthesis, where bioactive compounds from the plant extract (such as polyphenols and proteins) remain as a capping layer on the nanoparticle surface to provide steric stabilization and prevent agglomeration (Awwad *et al*., 2013). the XRD results obtained in this study are consistent with recent literature on biogenic nanostructures. The observed peak broadening (FWHM ≈ 1.46°) is a characteristic phenomenon for materials with nanoscale structures, where reduced crystallite dimensions lead to incomplete destructive interference at angles slightly off the Bragg condition (Stock, 2013).

According to Suryanarayana and Norton (1998), such shifts and broadening are common in nanostructured materials due to internal micro-strain and the high surface-to-volume ratio. Furthermore, the slight peak shift observed in the main peak position (33.45°) compared to the bulk ZnO standard is attributed to lattice strain and structural imperfections induced during the rapid biogenic reduction process. these findings are in strong agreement with Toma *et al*. (2025) and Krysova *et al*. (2024), confirming that the synthesis method successfully produced stable, crystalline ZnO nanoparticles capped with a functional organic shell.

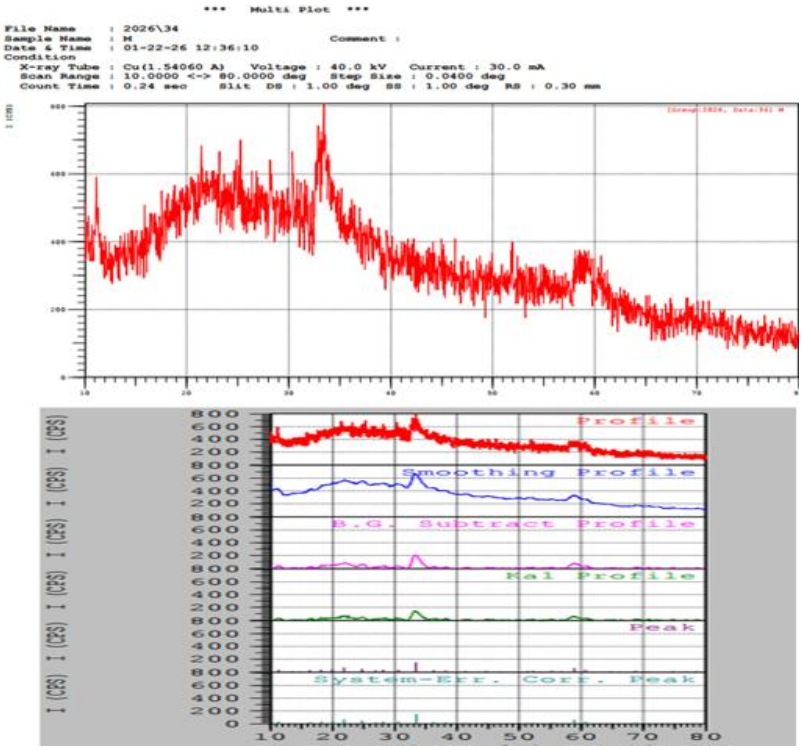

Figure (9): *X-ray diffraction (XRD) patterns of ZnoNPs*

Antibacterial activity of Moringa ZnO NPs on *Bacillus cereus*

In this study, the antibacterial synergistic efficacy of green-synthesized zinc oxide nanoparticles using Moringa oleifera extract, in combination with tetracycline, was investigated against a representative set of Bacillus cereus isolates isolated from clinical sources. *Bacillus cereus*, which consisted of a clinical isolate (M7). chosen for their unique colony morphologies, robust growth patterns, and corresponding antimicrobial susceptibility classifications that were determined during an extensive screening of all isolates in the laboratory. The standard antibiotic potencies as recommended by the Clinical and Laboratory Standards Institute (CLSI) were used to evaluate the antibacterial activity of both the ZnO-NPs and tetracycline at 30 μg were the selected antibiotic concentration for this investigation to ensure clinical relevance and standardization of interpretation of the synergistic interactions. Based on their different levels of antibacterial effectiveness against the tested *B. cereus* isolated during the preliminary susceptibility assay. tetracycline exhibited comparatively weak antibacterial activity and produced the lowest inhibition zones among the tested antibiotics. tetracycline provided an appropriate experimental model to investigate whether biogenic ZnO-NPs could enhance the antibacterial efficacy of agents with different intrinsic activities against *B. cereus*. The various ways that antibacterial activity occurs with ZnO-NPs include interaction with both bacterial cell wall as well as membrane which results in the disruption of the structural integrity of the bacteria, as well as the release of Zn^{2+} ions into the bacteria, where this release is disruptive to critical enzymatic systems, and, thirdly, the induction of the production of reactive oxygen species that disrupt and/or damage cellular proteins, lipids, nucleic acids, etc. (Al-Mashhadani, 2025; Mohammed *et al.*, 2025). the combination of tetracycline with biogenic ZnO-NPs demonstrated a pronounced and consistent synergistic effect against tested isolates. the inhibition zone of the clinical isolate M7 increased from 35 mm with tetracycline alone to 38 mm following nanoparticle addition.These findings indicate that ZnO-NPs significantly enhanced the antibacterial activity of tetracycline against *B. cereus* isolates with reduced susceptibility. Synergistic between tetracyclines and ZnO NPs may be explained by the combination of their respective mechanism of actions. Tetracycline acts primarily by binding to the 30S ribosomal subunit of bacteria and inhibiting protein synthesis in those organisms (Chopra and Roberts, 2001). The instance wherein resistance to tetracycline occurs in *B. cereus* is often attributed to decreased membrane permeability, active efflux pumps, or ribosomal protection proteins, which limit the accumulation of antibiotic within the cell. ZnO NPs may overcome the above-listed

Resistance mechanisms through several potential mechanisms:

disruption of the bacterial cell wall and membrane integrity, generation of reactive oxygen species (ROS), release of Zn2+ ions, and/or increased cell membrane permeability. The combination of these events is suspected to enhance the intracellular penetration of tetracycline into bacteria, thereby enhancing its inhibitory effects. Thus, biogenic ZnO-NPs synthesized with Moringa oleifera extract may act as effective nano-bioenhancers to increase the activity of conventional antibiotics against *B. cereus* (Sirelkhatim *et al.*, 2015). *B. cereus* spores possess highly resistant structural layers and reduced metabolic activity, their susceptibility to nanoparticles and antibiotics may differ significantly from that of vegetative cells. It is important to note that the observed antibacterial activity primarily reflects the effect of ZnO-NPs and antibiotics on vegetative bacterial cells rather than dormant spores. This is because the antimicrobial susceptibility testing was performed using actively growing bacterial cultures under standard CLSI conditions. Therefore, the present findings mainly demonstrate the effectiveness of ZnO-

NPs against actively proliferating *B. cereus* cells (Setlow, 2014).

Clinical (M7)	Treatment type	Concentration of ZNO
35mm	Antibiotic	5mg
15mm	ZNO	
38mm	ZNO+Antibiotic	
35mm	Antibiotic	2.5mg
12mm	ZNO	
37mm	ZNO+Antibiotic	
35mm	Antibiotic	1.25mg
10mm	ZNO	
36mm	ZNO+Antibiotic	

Table (3): *Antibacterial activity of moringa ZnO-NPs in combination with tetracycline against B. cereus isolates from clinical source*

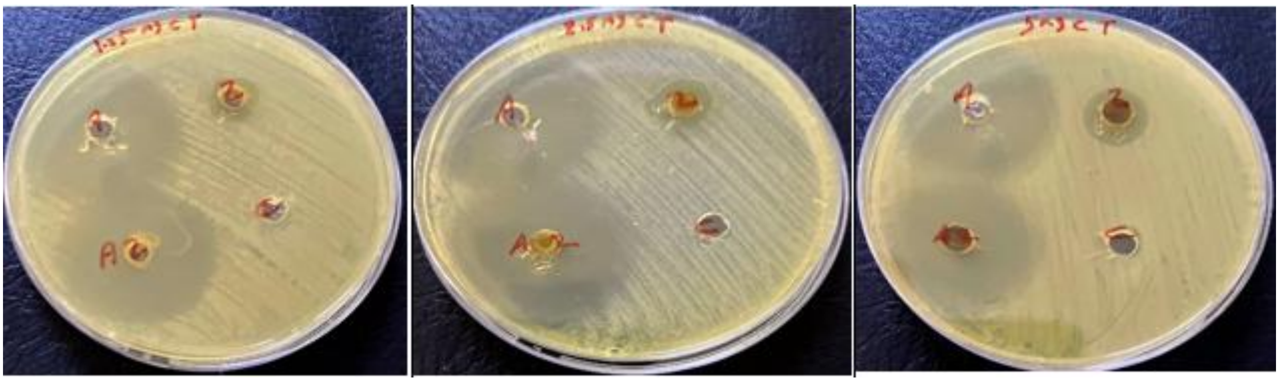

Figure (10): *Effect of different concentrations (5, 2.5, 1.25 mg/ml) of ZnO nanoparticles on the inhibition of Bacillus cereus*

These results agree with those reported by Sharmila *et al*. (2018), who observed enhanced antibacterial activity when tetracycline was combined with biogenic ZnO-NPs against several *Bacillus* species. Tetracycline acts by inhibiting bacterial protein synthesis through binding to the 30S ribosomal subunit; however, resistance mechanisms such as efflux pumps, reduced membrane permeability, and ribosomal protection proteins may limit its intracellular activity in *B. cereus*.

References:

1. Sharmila, G., Muthukumaran, C., Sandiya, K., Santhiya, S., Pradeep, R. S., Kumar, N. M., . . . Thirumarimurugan, M. (2018). Biosynthesis, characterization, and antibacterial activity of zinc oxide nanoparticles derived from Bauhinia tomentosa leaf extract. Journal of Nanostructure in Chemistry, 8(3), 293-299.
2. 20-Stock, S. (2013). Elements of X-ray diffraction: pearson new international edition PDF eBook: Pearson Higher Ed.
3. Setlow, P. (2014). Germination of spores of Bacillus species: What we know and do not know. Journal of Bacteriology, 196(7), 1297–1305.
4. Awwad, A. M., Salem, N. M.,&Abdeen, A. O. (2013). Green synthesis of silver nanoparticles using carob leaf extract and its antibacterial activity. International Journal of Industrial Chemistry, 4(1), 29.
5. Sirelkhatim, A., Mahmud, S., Seeni, A., Kaus, N. H. M., Ann, L. C., Bakhori, S. K. M., ...&Mohamad, D. (2015). Review on zinc oxide nanoparticles: Antibacterial activity and toxicity mechanism. Nano-Micro Letters, 7(3), 219–242.
6. Krysova, H., Mansfeldova, V., Tarabkova, H., Pisarikova, A., Hubicka, Z.,&Kavan, L. (2024). High-quality dense ZnO thin films: work function and photo/electrochemical properties. Journal of Solid State Electrochemistry, 28(8), 2531-2546.
7. Masum, M. M. I., Siddiqa, M. M., Ali, K. A., Zhang, Y., Abdallah, Y., Ibrahim, E., . . . Li, B. (2019). Biogenic synthesis of silver nanoparticles using Phyllanthus emblica fruit extract and its inhibitory action against the pathogen Acidovorax oryzae strain RS-2 of rice bacterial brown stripe. Frontiers in Microbiology, 10, 820.
8. Elumalai, K., Velmurugan, S., Ravi, S., Kathiravan, V.,&Ashokkumar, S. (2015). RETRACTED: Green synthesis of zinc oxide nanoparticles using Moringa oleifera leaf extract and evaluation of its antimicrobial activity. In: Elsevier.
9. Tiwari, V., Mishra, N., Gadani, K., Solanki, P., Shah, N.,&Tiwari, M. (2018). Mechanism of anti-bacterial activity of zinc oxide nanoparticle against carbapenem-resistant Acinetobacter baumannii. Frontiers in Microbiology, 9, 1218.
10. Moodley, J. S., Krishna, S. B. N., Pillay, K., Sershen, F.,&Govender, P. (2018). Green synthesis of silver nanoparticles from Moringa oleifera leaf extracts and its antimicrobial potential. Advances in Natural Sciences: Nanoscience and Nanotechnology, 9(1), 015011.
11. Suryanarayana, C.,&Norton, M. G. (1998). X-Ray Diffraction: A Practical Approach. Springer Science & Business Media.

12. Toma, F. T. Z., Rahman, M. S.,&Maria, K. H. (2025). A review of recent advances in ZnO nanostructured thin films by various deposition techniques. Discover Materials, 5(1), 60.
13. Mtavangu, S. G., Machunda, R. L., van der Bruggen, B.,&Njau, K. N. (2022). In situ facile green synthesis of Ag–ZnO nanocomposites using Tetradenia riperia leaf extract and its antimicrobial efficacy on water disinfection. Scientific Reports, 12(1), 15359.
14. Radulescu, D.-M., Surdu, V.-A., Ficai, A., Ficai, D., Grumezescu, A.-M.,&Andronescu, E. (2023). Green synthesis of metal and metal oxide nanoparticles: a review of the principles and biomedical applications. International Journal of Molecular Sciences, 24(20), 15397.
15. Jagadeesh, P., Rangappa, S. M.,&Siengchin, S. (2024). Advanced characterization techniques for nanostructured materials in biomedical applications. Advanced Industrial and Engineering Polymer Research, 7(1), 122-143.
16. Handore, K., Bhavsar, S., Horne, A., Chhattise, P., Mohite, K., Ambekar, J., . . . Chabukswar, V. (2014). Novel green route of synthesis of ZnO nanoparticles by using natural biodegradable polymer and its application as a catalyst for oxidation of aldehydes. Journal of Macromolecular Science, Part A, 51(12), 941-947.
17. Nakamoto, K. (2009). Infrared and Raman spectra of inorganic and coordination compounds, part B: applications in coordination, organometallic, and bioinorganic chemistry: John Wiley&Sons.
18. Verma, N., Rakhra, M., Bhatt, M. W.,&Garg, U. (2022). Engineering technology characterization of source solution for ZnO and their data analytics effect with aloe vera extract. Neuroscience Informatics, 2(3), 100015.
19. Ahmed, A. a. J.,&Alias, M. F. (2024). Synthesis, Spectroscopic, and Characterization of Novel Nano Sized Mannich Base Complexes with Pt (IV) and Au (III) Ions and Assessing Their Antioxidants Activity. Baghdad Science Journal, 21(10), 4.
20. Naveed, M., Din, M. S. U., Aziz, T., Asim, M., Makhdoom, S. I., Khan, A. A., ...&Alrayyani, M. A. (2025). Biosynthesis of cysteine-conjugated zinc oxide nanoparticles using secondary metabolites of Bacillus licheniformis for wastewater purification. Desalination and Water Treatment, 101370.
21. Al-Mashhadani, T. A. (2025). Investigating the antibacterial activity of zinc oxide nanostructures. Journal of Biological and Applied Research. https://jbaar.journals.ekb.eg/article_419993_661b6aeda6e9128589346b8337a58ef2.pdf?utm_source=chatgpt.com
22. Abdellatif, A., Mohammed, H., Abdulla, M., Alsubaiyel, A., Mahmood, A., Samman, W., ...&Vaali-Mohammed, M. (2023). Green synthesized silver nanoparticles using the plant-based reducing agent Matricaria chamomilla induce cell death in colorectal cancer cells. European Review for Medical&Pharmacological Sciences, 27(20).
23. Mohammed, T. D., Hadi, N. A., Risan, M. H., Saad, R. J.,&Mohammed, A. A. (2025). Green synthesis of zinc oxide nanoparticles using Aloe vera extract and antibacterial effects against Bacillus cereus. International Journal of Environmental Sciences, 11(16s). https://theaspd.com/index.php/ijes/article/download/3538/2643?utm_source=chatgpt.com
24. Woh, P. Y., et al. (2024). Bacillus cereus in rice: food poisoning, antimicrobial resistance, and control measures. Tropical Biomedicine, 41(3). https://msptm.org/files/Vol41No3/tb-41-3-010-Woh-P-Y.pdf?utm_source=chatgpt.com
25. Rao, J. P., Geckeler, K. E.,&Nguyen, T. A. (2021). Nanotechnology for drug delivery systems: An overview. Journal of Materials Chemistry B, 9(5), 1083–1098. https://doi.org/10.1039/D0TB02529A
26. Hassan, Z. A., and Risan, M. H. (2024). Green synthesis of zinc oxide nanoparticles and its antibacterial Activity on Pseudomonas aeruginosa. Jornal of Biotechnology Research Center, 18(2).
27. Jayachandran, A., T R, A., and Nair, A. S. (2021). Green synthesis and characterization of zinc oxide nanoparticles using Cayratia pedata leaf extract. Biochemistry and Biophysics Reports, 26, 100995. https://doi.org/10.1016/j.bbrep.2021.100995
28. Chopra, I.,&Roberts, M. (2001). Tetracycline antibiotics: Mode of action, applications, molecular biology, and epidemiology of bacterial resistance. Microbiology and Molecular Biology Reviews, 65(2), 232–260.
29. Hooper, D. C.,&Jacoby, G. A. (2015). Mechanisms of drug resistance: Quinolone resistance. Annals of the New York Academy of Sciences, 1354(1), 12–31.
30. Handore, K., Bhavsar, S., Horne, A., Chhattise, P., Mohite, K., Ambekar, J., ...&Chabukswar, V. (2014). Novel green route of synthesis of ZnO nanoparticles by using natural biodegradable polymer and its application as a catalyst for oxidation of aldehydes. Journal of Macromolecular Science, Part A, 51(12), 941-947.
31. Maria, A.,&Rahman, F. (2025). The impact of surface roughness on the functional performance of metal oxide nanostructures. Nanotechnology Reviews, 12(1), 45-58.
32. Mtavangu, S. G., Machunda, R. L., van der Bruggen, B.,&Njau, K. N. (2022). In situ facile green synthesis of Ag–ZnO nanocomposites using Tetradenia riperia leaf extract and its antimicrobial efficacy on water disinfection. Scientific Reports, 12(1), 15359.
33. Sirelkhatim, A., Mahmud, S., Seeni, A., Kaus, N. H. M., Ann, L. C., Bakhori, S. K. M., ...&Mohamad, D. (2015). Review on zinc oxide nanoparticles: Antibacterial activity and toxicity mechanism. Nano-Micro Letters, 7(3), 219–242